Systematic Optimization of a H_2 PEMFC Power Generation System with Heat Integration

Cong Xu, Lorenz T. Biegler, and Myung S. Jhon
Department of Chemical Engineering
Carnegie Mellon University
Pittsburgh, PA 15213

ABSTRACT

We examine a H_2 PEMFC power generation system composed of three subsystems: fuel reforming, fuel cell stack, and post combustion. The system was simulated and optimized with a fuel cell model integrated within the process flow sheet. We present a case study of the H_2 production optimized w.r.t. the CH_4 and H_2O inlet flow rate and the temperature of steam methane reform reactor. Our objectives are to maximize the system efficiency，minimize the operating cost or maximize the profit. In addition, optimization formulations with heat integration are used to realize our objectives. Our results showed that we can achieve a system efficiency as high as 57.2% at an optimal steam to carbon ratio of 4:1. Also, we obtained about 1 percent higher efficiency for the case with heat integration than without it. On the other hand, the effect of heat integration is much more significant in the minimum utility cost case, as the utility cost is almost tripled without heat integration.

KEY WORDS

Fuel Cell System; H_2 PEM Fuel Cell; Heat Integration; Power Generation; Efficiency; Cost Optimization.

Introduction and background

Fuel cells have recently attracted considerable attention as a potential replacement for current power generation and automobile engine systems. Fuel cells have the advantage of high power density, high efficiency, and zero or ultra-low emissions and promise to ease concerns regarding fossil energy and environment. Government and the industry supported research programs have concentrated on the development the operable fuel cells and their commercialization. In a “fuel cell report to Congress”(Garman 2003), cost and durability are the primary technical barriers to commercialization. To reduce the cost and improve the durability of the fuel cells, we need to understand the fuel cell at every level such that we can provide an optimal design accordingly. Since the modeling work should reflect the complexity of the overall process, unravel the interactions, and simplify input/output characteristics of components(Gemmen and Selman 2000), the National Energy Technology Laboratory (NETL) is currently developing a multi-level model of fuel cells, including the micro or fundamental modeling, cell modeling, stack modeling, and system modeling. There are many publications(Fuller and Newman 1993; Nguyen and White 1993; Springer et al. 2001; Springer et al. 1991; Um and Wang 2004; Wang and Wang 2003) about fuel cell modeling. Starting from the early 90s, researchers(Bernardi and Verbrugge 1992; Fuller and Newman 1993; Nguyen and White 1993; Springer et al. 1991) have begun to develop fuel cells models. They started from simple 0-D models, some of which focused on separate parts in the fuel cells, *e.g.*, the electrodes or the gas diffusion layers(Bernardi and Verbrugge 1992). Recently, Springer(Springer et al. 2001) developed a 1-D H_2 PEMFC model which examines the effect of CO poisoning and hydrogen dilution. Wang and coworkers have modeled PEMFCs extensively and have extended the model to two(Wang and Wang 2003) and even three spatial dimensions(Um and Wang 2004). Water and heat management have also been considered in their models since the temperature profiles can be easily obtained with high-dimensional models by incorporating computation fluid dynamics (CFD) techniques. Despite the rapid development of fuel cell modeling, there are few studies on fuel cell systems including fuel reforming processes. To reduce the cost and improve the performance, it will be desirable to examine fuel cell behavior under the environment of the whole process. We not only need to understand cells and stacks, but also the supporting technology relevant to fuel cell development, *e.g.*, fuel storage, fuel distribution, fuel reforming, post-combustion, and heat exchanger networks. Moreover, optimization has been in high demand for fuel cell design and operation. Since the late 90s, Moore and coworkers (1998) have been working on the optimization of the overall energy conversion efficiency and concentrated on performance of DMFC stacks in automotive applications. They aimed to develop an operational strategy to achieve the maximum efficiency by varying the methanol feed concentration and flow rate under a wide range of power demands. Similarly, we have recently performed an optimization study on a DMFC, which provides methanol feeding strategies both in the steady and dynamic states

to achieve the maximum power output under various current densities(Xu et al. Submitted). Godat and Marechal (2003) considered the effect of heat integration of the performance of power generation systems that incorporate H_2 PEM fuel cells. Similarly, this study focuses on the optimization of a particular heat integrated PEM fuel cell power generation system. Quantitative results and heat exchanger network (HEN) structures are presented in our optimization study to provide guidance for the operation of the system.

The fuel cell system

Our system model is based on the work by Godat and Marechal (2003) and builds a flow sheet using the Aspen Plus (Aspen User's Guide, 2001) simulator as shown in Figure 1. The fuel cell system is composed of three subsystems as follows:

(1) The fuel processing (FP) subsystem.
(2) The PEMFC stack subsystem.
(3) The post-combustion subsystem.

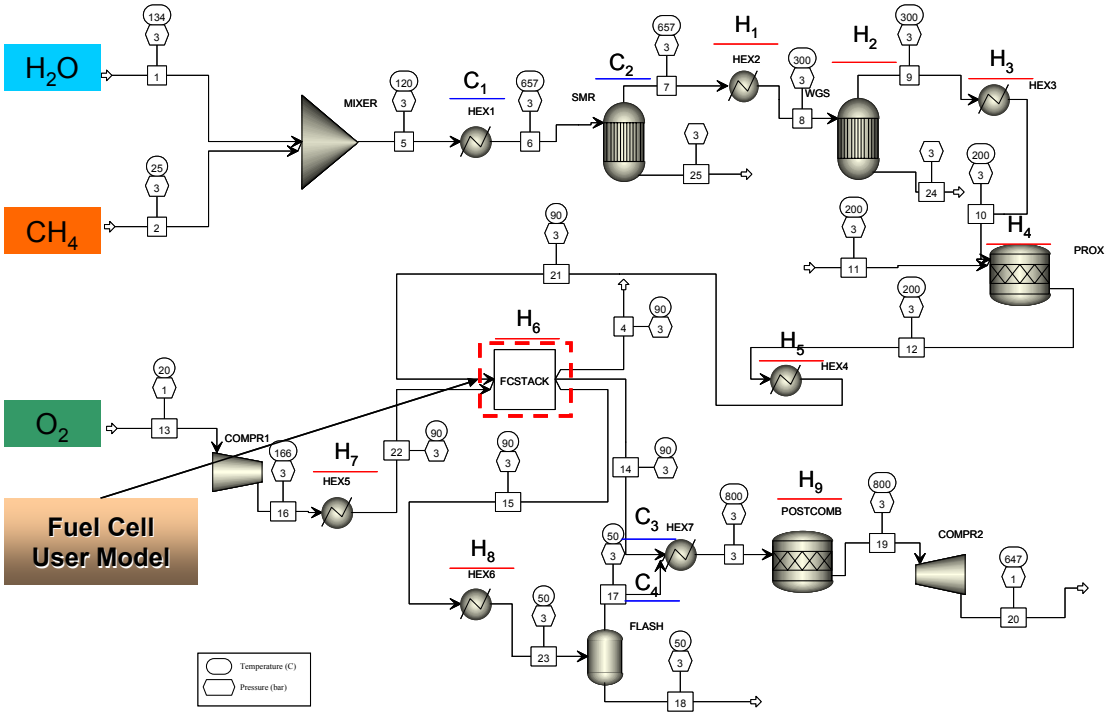

Figure 1. The ASPEN Plus flow sheet for the fuel cell system with temperature and pressure displayed for each stream.

Stream #1 is saturated steam feed at 3 bar and stream #2 is a pure methane feed provided at 3 bar and 25 °C. The two streams are combined, heated to reactor temperature and fed to the steam methane reforming (SMR) reactor, where methane and steam are reacted on a catalyst surface to produce hydrogen and carbon monoxide. The effluent from the SMR reactor enters the water gas shift (WGS) reactor, where carbon monoxide reacts further with steam to produce hydrogen and carbon dioxide. Both of these two reactions are assumed to be at equilibrium. Afterwards, the WGS effluent enters the preferential oxidation reactor along with stream #11 to oxidize the remaining CO in the stream. Stream #11 is a pure oxygen flow required for the oxidation of CO. The effluent stream from the preferential oxidation (PROX) reactor, which is hydrogen-rich with trace amounts of CO, is fed to the anode of the fuel cell stacks. A compressed oxygen stream is fed to the cathode of the fuel cell stacks. The outlet stream from the anode is a hydrogen-lean stream, while the cathode effluent contains both O_2 and H_2O. After removing H_2O in a flash separator, the O_2 stream combines with the anode effluent and enters post-combustor where O_2 reacts with H_2. Finally the hot outlet stream from the post combustor is depressurized and discharged to the atmosphere.

The SMR and WGS reactors are both modeled with equilibrium reactor models (REquil) in ASPEN Plus. Reactions in the PROX and post-combustion (POSTCOMB) reactors essentially go to completion and are both modeled with the stoichiometric model (RStoic) in ASPEN Plus. All reactors are operated under isothermal conditions and heat is supplied or removed to maintain the temperature in the reactor from an external hot or cold utility. In order to define appropriately the energy requirement of the heat exchange, we have assumed that the inlet streams are preheated up to the reaction temperature. To model them, we place heat exchangers before each unit to ensure that the inlet stream is at the same temperature. The use of process integration techniques allows us to avoid the detailed calculation of the complex heat exchange network within the heat integrated system.

Heat integration

The idea of simultaneous optimization and heat integration of chemical processes was initially proposed by Grossmann et al.(Duran and Grossmann 1986). Later on, Lang et al.(Lang et al. 1988) and Yee et al.(Yee et al. 1990) improved this approach and expanded its application for process design and with flowsheet simulators. The heat exchange network has not been considered directly in the simulation model described above. Instead, pinch technology can be used to model the integrated heat exchange system without having to impose a heat exchange network structure. A typical heat integration optimization problem using pinch technology can be described as follows(Biegler et al. 1997):

$$\min C = \phi(x) + c_H Q_H + c_C Q_C$$

$$s.t. \quad h(x) = 0$$

$$g(x) \le 0$$

$$Q_H \ge \sum_{j=1}^{n_c} f_j [\max\{0, t_j^{out} - (T^p - \Delta T_{\min})\} - \max\{0, t_j^{in} - (T^p - \Delta T_{\min})\}] \quad (1)$$

$$- \sum_{i=1}^{n_H} F_i [\max\{0, T_i^{in} - T^p\} - \max\{0, T_i^{out} - T^p\}], \mathrm{p} \in \Pi$$

$$Q_C = Q_H + \Omega$$

$$\Omega = \sum_{i=1}^{n_H} F_i (T_i^{in} - T_i^{out}) - \sum_{j=1}^{n_C} f_i (t_j^{out} - t_j^{in})$$

where $\phi(x)$ is the cost/profit function other than utility cost, Ω is the heat surplus of the system, Q_H is the requirement of the hot utility, Q_C is the requirement of the cold utility, *h(x)* is the ASPEN Plus flow sheet model, *g(x)* represents the inequality constraints, *j* is the index for cold streams in the flow sheet, *i* is the index for hot streams, t_j is the temperature of cold stream *j*, T_i is the temperature of hot stream *i*, F_i and f_j are the heat capacity flowrates for the hot and cold streams, respectively. The set defines candidate pinch points and T_p , $p \in \Pi$ is the candidate pinch temperature defined as follows:

$$T^P = \begin{cases} T_i^{in} & \text{if candidate } p \text{ is hot stream } i \\ t_j^{in} + \Delta T_{\min} & \text{if candidate } p \text{ is cold stream } j \end{cases} \quad (2)$$

$\Delta T_{\min}$ is the minimal approach temperature that is possible for the heat exchange to take place, which is set to be 20 °C in our study. The number of pinch temperature candidates is determined by the total number of hot and cold streams. The right hand side of the inequality for Q_H in Eq. (2) represents the difference between the heat contents of the cold and hot streams (heat deficit) above any candidate pinch $p \in \Pi$. The problem is then posed to find the minimal value of Q_H such that all the inequalities hold; Q_H therefore equals the maximal value of the heat deficit and the temperature T^p where the heat deficit achieves this maximum is the pinch point.

Note that the above formulation can treat the flows and the temperatures as variables for the optimization and the heat integration. The remaining difficulty is the presence of nondifferentiable max operators in Eq. (2). As shown in Eq. (4), a smoothing approximation procedure can be used that avoids difficulties with the use of NLP solvers(Balakrishna and Biegler 1992).

$$\max\{0, f(x)\} = 0.5\left[f(x)^2 + \varepsilon^2\right]^{1/2} + 0.5 f(x) \quad (3)$$

where ε usually assumes a relatively small value (*e.g.*, 10^{-3} in our study).

Results and Discussion

Efficiency analysis

We first focus on the efficiency. There are two efficiencies to evaluate the system: one is the energy efficiency and the other is the system efficiency. The energy efficiency only considers the conversion rate of the fuel source energy to the cell power, which can be defined as follows:

$$\eta_{energy} \equiv \frac{P_{cell}}{P_{combusion}} \equiv \frac{V_{cell} \cdot I_{cell}}{f_{CH_4} \cdot LHV_{CH_4}} \quad (4)$$

where LHV_{CH4} denotes the lower heating value of methane.

The system efficiency can be defined as:

$$\eta_{FCsys} \equiv \frac{P_{cell}}{P_{combusion}} \equiv \frac{V_{cell} \cdot I_{cell}}{f_{CH_4} \cdot LHV_{CH_4} + Q} \qquad (5)$$

Where Q is the additional energy consumed to operate the system. This quantity consists mostly of the hot and cold utilities.

Optimal energy efficiency

The optimization problem can be defined as follows:

$$\max_{\{f_{CH_4}^{In}, T_{SMR}\}} \quad \eta_{energy} = \frac{P_{cell}(f_{CH_4}, T_{SMR}, y)}{LHV_{CH_4} \cdot f_{CH_4}}$$
$$s.t. \quad h(f_{CH_4}, T_{SMR}, y) = 0$$
$$50 \le f_{CH_4} \le 200;$$
$$420 \le T_{SMR} \le 780;$$
$$200 \le T_{SMR} \le 400. \qquad (6)$$

where the equation $h(f_{CH4}, T_{SMR}, y) = 0$ represents the ASPEN Plus flow sheet model. The lower and upper bounds for f_{CH4} and T_{SMR} were chosen according to the results obtained from the sensitivity analysis. The range of T_{SMR} is determined from the thermodynamic analysis of the hydrogen production by steam reforming(Lutz et al. 2003).

As is shown in Table 1, optimal energy efficiency can be as high as 58.3% in our study when f_{CH4} assumes the lower bound value of 50 kmol/hr and T_{SMR} at the upper bound, 780 °C. As the CH_4 inlet rate increases, the energy efficiency decreases sharply before it reaches 100 kmol/hr and levels off afterwards. The optimal T_{SMR} also decreases accordingly until it reaches a lowest value at 627 °C.

Table 1. Energy efficiency optimization results for cases where f_{CH4}. assumes five different lower bounds respectively (* denotes optimal).

f^*_{CH4} (kmol/hr)	T^*_{SMR} (°C)	T^*_{WGS} (°C)	Pcell (kW)	Effi'y
50.00	780.00	236.44	6505.76	58.30%
80.00	679.00	244.81	6714.02	37.60%
100.00	655.48	245.85	6701.60	30.03%
120.00	647.87	250.84	6673.95	24.92%
150.00	627.52	252.27	6664.47	19.91%

System efficiency

By considering the heat and cold utility consumption in the whole system, we get the overall efficiency of the power generation system. This can be denoted as the cell power over the total of the fuel and utility energy consumption. Similar to the energy efficiency case, we can formulate the system efficiency optimization problem as follows:

$$\max_{\{f_{CH_4}^{In}, T_{SMR}\}} \quad \eta_{FCsys} = \frac{P_{cell}(f_{CH_4}, T_{SMR}, y)}{LHV_{CH_4} \cdot f_{CH_4} + Q_H + Q_C}$$
$$f(f_{CH_4}, T_{SMR}, y) = 0$$
$$s.t. \quad 50 \le f_{CH_4} \le 200;$$
$$420 \le T_{SMR} \le 780;$$
$$200 \le T_{WGS} \le 400. \qquad (7)$$

Here Q_H and Q_C result from the heat integration.

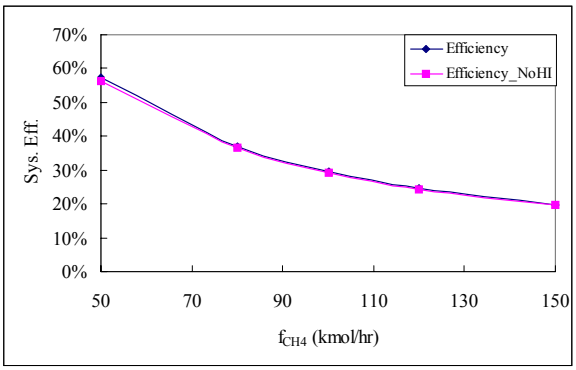

Figure 2. Comparison of the optimal system efficiency for the cases with and without heat integration.

Compared to energy efficiency, the optimal value of the system efficiency is correspondingly lower due to the consideration of the utility consumption, as is shown in Table 2. The maximal system efficiency is about 57.2%. The corresponding CH_4 inlet flow rate, T_{SMR}, and T_{WGS} are 50 kmol/hr, 780 °C and 200 °C, respectively. The lower bound can be explained because the f_{CH4} term appears in the denominator of the efficiency, which has a dominant effect on the objective value. T_{SMR} and T_{WGS} hit upper and lower bounds, respectively, due to the fact that SMR and WGS are endothermic and exothermic reactions. As the bound on CH_4 inlet flow rate is increased, the optimal system efficiency declines significantly, as shown in Figure 6. Also from Table 3, we can see that heat integration improves the system efficiency by at most 1% for various CH_4 inlet cases.

Table 2. System efficiency optimization results with heat integration (results are listed for cases where f_{CH4}. assumes five different lower bounds respectively).

f^*_{CH4} (kmol/hr)	T^*_{SMR} (°C)	T^*_{WGS}(°C)	P_{cell} (kW)	Q_H (kW)	Q_C (kW)	Efficiency
50.00	780.00	200.00	6510.02	108.58	109.02	57.22%
80.00	681.36	276.52	6715.13	162.41	168.64	36.92%
100.00	655.34	257.76	6701.57	175.92	168.78	29.57%
120.00	639.56	278.40	6688.57	190.45	182.33	24.63%
150.00	622.64	283.39	6670.70	211.83	194.52	19.69%

Table 3. System efficiency optimization results without heat integration.

f^*_{CH4} (kmol/hr)	T^*_{SMR} (°C)	T^*_{WGS}(°C)	Pcell (kW)	Qgen (kW)	Qsink (kW)	TotalQ (kW)	Efficiency _NoHI
50.00	780.00	200.00	6510.02	201.14	200.70	401.84	56.31%
80.00	681.36	276.52	6715.13	278.40	272.17	550.57	36.48%
100.00	655.34	257.76	6701.57	283.17	290.32	573.49	29.27%
120.00	639.56	278.40	6688.57	301.07	309.18	610.25	24.42%
150.00	622.64	283.39	6670.70	319.86	337.16	657.02	19.54%

Cost and profit optimization

Similar to the efficiency analysis, there are two different objectives to be optimized in the system: one is the utility cost, and the other is the system profit.

Utility cost

The utility cost only includes the cost of the hot and cold utilities consumed in the system. For cost coefficients, refer to Table 4. The problem can be formulated as follows:

$$\min C = c_H Q_H + c_C Q_C$$

$$s.t. \qquad h(x) = 0$$

$$g(x) \le 0$$

$$Q_H \ge \sum_{j=1}^{n_c} f_j [\max\{0, t_j^{out} - (T^p - \Delta T_{\min})\} - \max\{0, t_j^{in} - (T^p - \Delta T_{\min})\}] - \sum_{i=1}^{n_H} F_i [\max\{0, T_i^{in} - T^p\} - \max\{0, T_i^{out} - T^p\}], p \in P \qquad (8)$$

$$Q_C = Q_H + \Omega;$$

$$\Omega = \sum_{i=1}^{n_H} F_i (T_i^{in} - T_i^{out}) - \sum_{j=1}^{n_C} f_j (t_j^{out} - t_j^{in});$$

$$50 \le f_{CH_4} \le 200;$$

$$420 \le T_{SMR} \le 780;$$

$$200 \le T_{WGS} \le 400.$$

Table 4. Cost coefficients (IChemEGroup, 2002) values for the system. (C_H is for hot utility, *i.e.*, natural gas, C_C is for the cold water utility, C_p is for the power output, C_{CH4} is for the CH_4 inlet stream)

Cost coeffi.	C_H ($/kWh)	C_C ($/kWh)	Cp ($/kWh)	C_{CH4} ($/kmol)
Value	0.0147	0.0017	0.0921	2.8739

As shown in Table 5, both the optimal CH_4 inlet flow rate and the T_{SMR} achieve their lower bounds as less utility is needed to operate the system. However, T_{WGS} did not assume the lower bound value. Above all, this study provides an illustration on how important and effective the heat integration is for our optimization. As is shown in Table 6, the minimum utility cost without heat integration is tripled for a lower bound at 50 kmol/hr CH_4 inlet flow rate and more than doubled for a lower bound at 150 kmol/hr.

Table 5. Optimal utility cost with heat integration (results are for cases where f_{CH4}. assumes three different lower bounds, where * denotes optimal.)

f^*_{CH4} (kmol/hr)	T^*_{SMR} (°C)	T^*_{WGS} (°C)	P_{cell} (kW)	System Efficiency	Q_H (kW)	Q_C (kW)	Cost ($/hr)
50.00	420.00	279.61	1980.60	17.71%	12.02	12.72	0.20
100.00	420.00	312.39	2411.18	10.78%	21.59	18.82	0.35
150.00	420.00	334.43	2724.37	8.12%	32.53	25.21	0.52

Table 6. Utility cost without heat integration.

f^*_{CH4} (kmol/hr)	T^*_{SMR} (°C)	T^*_{WGS} (°C)	P_{cell} (kW)	System Efficiency	Q_H (kW)	Q_C (kW)	Cost_NoHI ($/hr)
50.00	420.00	279.61	1980.60	17.64%	36.24	35.55	0.60
100.00	420.00	312.39	2411.18	10.75%	49.96	52.73	0.83
150.00	420.00	334.43	2724.37	8.11%	63.26	70.58	1.05

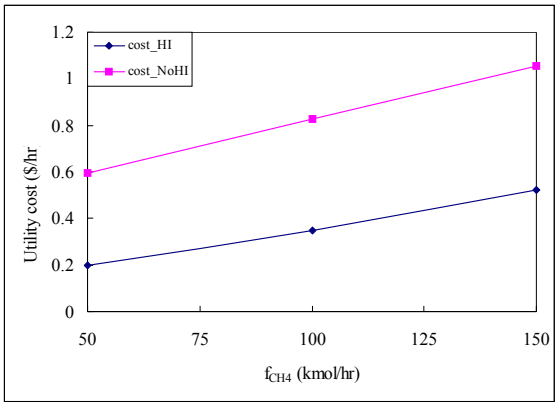

Figure 3. Comparison of the minimal utility cost for cases with and without heat integration.

System profit

The total system profit equals the revenue from the power generated by the fuel cell stack minus utility cost and the cost of the material (methane only). The corresponding minimization problem can be represented in Eq. (9).

Note from Table 7 that the optimal values for the decision variables differ a lot from the minimization of the utility cost case. We found that the power revenue and material cost are several orders of magnitude larger than the utility cost. Thus, the utility cost term doesn't play a significant role in the objective function. This explains why the optimization results for the decision variables are so different in both cases. We initially set the lower bound of f_{CH4} to be 50.0. We got the optimal f_{CH4} to be 52.59 kmol/hr, which is closer to bound. Then we lift the lower bound in the following two cases, *i.e.*, 100.0 and 150.0 kmol/hr respectively. As expected, the optimal f_{CH4} hits the lower bound in both cases. The methane cost occupies approximately 25% of the revenue when f_{CH4} is around 50.0 kmol/hr; as we increase the lower bound of f_{CH4}, the cost percentage for methane increases tremendously. This contributes to the reason why the optimal value of f_{CH4} hit the lower bound. And we observe a sharp decrease in the profit. From these results, we can conclude that a steam to carbon ratio of approximately 4:1 might be the optimal operating condition for this system, since we not only achieve largest profit, but almost the highest efficiency (56.21% in this case). For comparison purposes, the system cost without heat integration was listed in Table 8. The corresponding curves are shown in Figure 11. We didn't observe a significant decrease of the profit. However, if we compare the utility requirement only, the total utility is lowered approximately 40% for the case with heat integration. This is the key contribution from heat integration.

$$
\begin{aligned}
&\min C = c_H Q_H + c_C Q_C - c_p P_{cell} + c_{CH_4} f_{CH_4} \\
&s.t. \qquad h(x) = 0 \\
&\qquad\quad g(x) \le 0 \\
&Q_H \ge \sum_{j=1}^{n_c} f_j [\max\{0, t_j^{out} - (T^p - \Delta T_{\min})\} \\
&\qquad - \max\{0, t_j^{in} - (T^p - \Delta T_{\min})\}] \\
&- \sum_{i=1}^{n_H} F_i [\max\{0, T_i^{in} - T^p\} \\
&\qquad - \max\{0, T_i^{out} - T^p\}] \\
&Q_C = Q_H + \Omega; \\
&\Omega = \sum_{i=1}^{n_H} F_i (T_i^{in} - T_i^{out}) - \sum_{j=1}^{n_C} f_j (t_j^{out} - t_j^{in}).
\end{aligned}
\tag{9}
$$

Table 7. System profit optimization results with heat integration (Results are listed for cases where the lower bound for f_{CH4}. was set to be 50.00, 100.00 and 150.00 respectively).

f^*_{CH4} (kmol/hr)	T^*_{SMR} (°C)	T^*_{WGS} (°C)	P_{cell} (kW)	System Efficiency	Q_H (kW)	Q_C (kW)	Profit ($/hr)
52.59	780.00	200.00	6597.14	55.10%	117.84	117.72	454.39
100.00	660.44	335.73	6701.46	29.51%	183.23	210.67	326.61
150.00	627.13	352.03	6670.49	19.65%	219.94	241.52	179.46

Table 8. System profit optimization results without heat integration.

f^*_{CH4} (kmol/hr)	T^*_{SMR} (°C)	T^*_{WGS} (°C)	P_{cell} (kW)	System Efficiency	Q_H (kW)	Q_C (kW)	Profit_NoHI ($/hr)
52.59	780.00	200.00	6597.14	54.24%	213.16	213.28	452.82
100.00	660.44	335.73	6701.46	29.21%	325.65	298.20	324.36
150.00	627.13	352.03	6670.49	19.51%	367.35	345.77	177.11

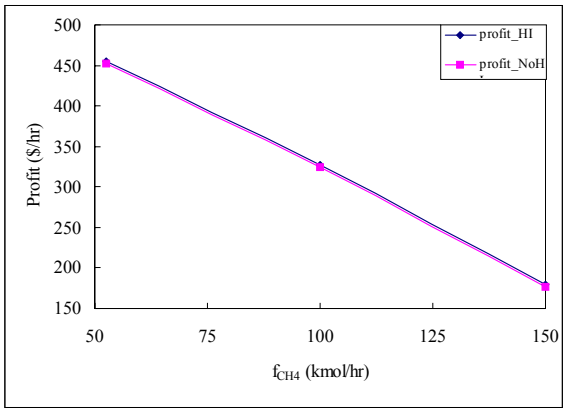

Figure 4. Comparison of the profit for cases with and without heat integration.

Conclusions

We carried out the simulation and optimization of a typical power generation system using ASPEN Plus. The CH_4 inlet flow rate, the WGS reactor temperature and the temperature of the SMR reactor are the main decision variables in our study. The optimization is concentrated on high efficiency and cost minimization, which are goals of the current fuel cell development. We also performed a sensitivity case study on the fuel cell performance characterized by the power output.

To generalize our model, a more complicated fuel cell model is needed. Also, the capital costs of the process flowsheet and heat integration network were not considered, which might influence our simulation and optimization results. Also, to determine the best selection of the HEN a mixed integer nonlinear programming (MINLP) formulation should be applied.

Acknowledgements

PITA (Pennsylvania Infrastructure and Technology Alliance) administered by the Institute of Complex Engineered Systems (ICES) at Carnegie Mellon University is gratefully acknowledged for the financial support of this project.

Literature Cited

Aspen Plus Documentation Version 11.1, Aspen Technology, Inc.(2001).

Balakrishna, S. and L. T. Biegler, "Targeting Strategies for the Synthesis and Energy Integration of Nonisothermal Reactor Networks." *Ind Eng Chem Res,* **31**, 2152 (1992).

Bernardi, D. M. and M. W. Verbrugge, "A Mathematical Model of a Gas Diffusion Electrode Bonded to a Polymer Electrolyte." *AIChE Journal,* **37**, 2477 (1992).

Biegler, L. T., I. E. Grossmann and A. W. Westerberg, *Systematic Methods for Chemical Process Design*, Prentice Hall. NJ (1997).

Duran, M. A. and I. E. Grossmann, "Simultaneous Optimization and Heat Integration of Chemical Processes." *AICHE Journal,* **32**, 123 (1986).

Friedman, D. J. and R. M. Moore, Optimum Operating Curves for Fuel Cell Systems. Record of the 1st Annual Fuel Cell Vehicle Technology Conference, University of California, Davis, CA (1998).

Fuller, T. F. and J. Newman, "Water and Thermal Management in Solid Polymer Electrolyte Fuel Cells." *Journal of Electrochemical Society,* **140**, 1218 (1993).

Garman, D. K. Fuel Cell Report to the Congress (Esecs Ee-1973) (2003).

Gemmen, R. S. and J. R. Selman, Speeding the Progress of Fuel Cell Development. Proceedings of the NETL

Workshop on Fuel Cell Modeling, Morgantown, WV (2000).
Godat, J. and F. Marechal, "Optimization of a Fuel Cell System Using Process Integration Techniques." *Journal of Power Sources,* **118**, 411 (2003).
IES Group, "Process Utilities Cost Guide 2002." *http://ed.icheme.org/costutil.html,* (2002).
Lang, Y. D., L. T. Biegler and I. E. Grossmann, "Simultaneous Optimization and Heat Integration with Process Simulators." *Computers and Chemical Engineering,* **12**, 311 (1988).
Lutz, A. E., R. W. Bradshaw, J. O. Keller and D. E. Witmer, "Thermodynamic Analysis of Hydrogen Production by Steam Reforming." *International Journal of Hydrogen Energy,* **28**, 159 (2003).
Nguyen, T. V. and R. E. White, "A Water and Heat Management Model for Proton Exchange Membrane Fuel Cells." *Journal of Electrochemical Society,* **140**, 2178 (1993).
Springer, T. E., T. Rockward, T. A. Zawodzinski and S. Gottesfeld, "Model for Polymer Electrolyte Fuel Cell Operation on Reformate Feed: Effects of Co, H2 Dilution, and High Fuel Utilization." *Journal of Electrochemical Society,* **148**(1), A11 (2001).
Springer, T. E., T. A. Zawodzinski and S. Gottesfeld, "Polymer Electrolyte Fuel Cell Model." *Journal of Electrochemical Society,* **138**, 2334 (1991).
Um, S. and C. Y. Wang, "Three-Dimensional Analysis of Transport and Electrochemical Reactions in Polymer Electrolyte Fuel Cells." *Journal of Power Sources,* **125**, 40 (2004).
Wang, Z. H. and C. Y. Wang, "Mathematical Modeling of Liquid-Feed Direct Methanol Fuel Cells." *Journal of Electrochemical Society,* **150**, A508 (2003).
Xu, C., P. M. Follmann, L. T. Biegler and M. S. Jhon, "Numerical Simulation and Optimization of a Direct Methanol Fuel Cell." (Submitted to Computers and Chemical Engineering).
Yee, T. F., I. E. Grossmann and Z. Kravanja, "Simultaneous Optimization Models for Heat Integration. Iii. Optimization of Process Flowsheets and Heat Exchanger Networks." *Computers and Chemical Engineering,* **14**, 1185 (1990).

CONTACT

Cong Xu

cxu@andrew.cmu.edu

412-2682238(O)

Aug. 2000-present, Ph.D. Candidate, Department of Chemical Engineering, Carnegie Mellon University.

Sep. 1996-Jul. 2000, Department of Chemical Engineering, Tsinghua University, Beijing, China.